

# Exploration via Sample-Efficient Subgoal Design

Yijia Wang, Matthias Poloczek, Daniel R. Jiang

July 3, 2022

## Abstract

The problem of exploration in unknown environments continues to pose a challenge for reinforcement learning algorithms, as interactions with the environment are usually expensive or limited. The technique of setting subgoals with an intrinsic shaped reward allows for the use of supplemental feedback to aid an agent in environment with sparse and delayed rewards. In fact, it can be an effective tool in directing the exploration behavior of the agent toward useful parts of the state space. In this paper, we consider problems where an agent faces an unknown task in the future and is given prior opportunities to “practice” on related tasks where the interactions are still expensive. We propose a one-step Bayes-optimal algorithm for selecting subgoal designs, along with the number of episodes and the episode length, to efficiently maximize the expected performance of an agent. We demonstrate its excellent performance on a variety of tasks and also prove an asymptotic optimality guarantee.

## 1 Introduction

We study the problem of exploration in reinforcement learning (RL), where agents face the often expensive problem of exploring various regions of the state space in order to find a reasonable operating policy for the Markov decision process (MDP). In this paper, we examine the issue of exploration through a new lens, by focusing on problems with the following unique features: (1) there exists a distribution of possible environments (or tasks) that are related through common state and action spaces; (2) the agent must attain a sparse and delayed reward, such as reaching a goal; and finally, (3) interactions with the environment(s) are limited or expensive, in both training and testing. More specifically, we assume that there is a *training phase*, where the agent is given a fixed number of opportunities to train in randomly drawn environments (henceforth, we refer to these as

training environments), with the caveat that each interaction with the training environment incurs a cost. After these opportunities are exhausted, the agent enters a random *test environment* and must learn a policy given only a limited number of interactions. The idea is that the agent can learn an exploration strategy that works well on average, across the distribution of test environments, by practicing in related settings. Features (2) and (3) comprise of the standard motivation for finding an effective exploration strategy that can direct the agent to take actions towards valuable states.

The motivation for this problem class comes from a need to apply RL algorithms in real-world settings where fast and cheap interactions with the environment are not available and only a limited number of environments (or experiments) can be tried. The examples below illustrate two potential application domains of this problem setting.

1. Autonomous robotic systems have long been used to explore unknown or dangerous terrains, including meteorite search in Antarctica (Apostolopoulos et al., 2001), exploration of abandoned mines (Ferguson et al., 2004; Thrun et al., 2004), and navigation of terrains on Mars (Matthies et al., 1995). Offline policies are the norm in these situations, but it may be beneficial to introduce agents that execute an offline-learned exploration policy to guide the learning of an *online* policy that can better tailor to the details of the test environment. Matthies et al. (1995) describe the design of a rover for the Mars Pathfinder mission, where one of the main tasks is navigating the rover in a rocky terrain and reach a goal. To train for the eventual mission, the engineers utilized an “indoor arena” filled with specially selected rocks to act as obstacles, with sizes drawn from estimated distributions matching that of Martian terrains. Like our proposed framework, both the training and test environments are costly and the training environments are approximations of the eventual test environment, Mars.
2. Our second example is the potential for adaptive controllers for *carbon nanotube growth* (Nikolaev et al., 2014; Dee et al., 2018). Material scientists perform extensive experiments to find growth recipes (i.e., a designation of temperature adjustments, gas flow rates, etc) in order to optimize the growth rate of carbon nanotube forests. Such experimentation is time-consuming and can substantially increase the cost for labor and materials. Moreover, each new experiment may take place in slightly different laboratory environments. Research into *adaptive* controllers (i.e., recipes that adjust based on observing the current state of growth) there-

fore critically depend on sample-efficient training, which might be realized through additional reward signals.

**Main Contributions.** We make the following contributions toward sample-efficient exploration of *random environments* in reinforcement learning.

1. We propose a novel way of parameterizing exploration strategies that enhances a given subgoal design with potential-based reward shaping (PBRS). This “shaped-subgoal” approach is interpretable and allows the algorithm designer to encode intuition and structural insights. PBRS provides dense rewards to rapidly speed up learning while reducing the number subgoals required. Our approach achieves low-dimensional parameterizations of the space of exploration strategies. The dimensionality of the parameter space depends only on the number of subgoals and their parameterization rather than the size of the environments.
2. In order to understand the space of shaped-subgoal exploration strategies, we propose a tailored probabilistic model that learns the typical performance of subgoals from observations. More specifically, we model the expected performance (across the distribution of environments) of an underlying RL algorithm given  $\tau$  iterations when using a shaped-subgoal design  $\theta$ . In other words, we model the training curve for every  $\theta$  and quantify our uncertainty at every point via probabilistic inference. The approach is applicable for any underlying RL algorithm, and also works when there are an infinite number of possible tasks.
3. We propose a one-step Bayes-optimal approach to find an optimal shaped-subgoal exploration strategy that explicitly quantifies the trade-off between running a longer trial versus more replications of shorter trials in any given test environment. The motivation is that, given  $\tau_1 < \tau_2$ , an accurate evaluation of a particular design  $\theta$  after  $\tau_1$  steps may be more informative than a noisy evaluation of  $\theta$  after  $\tau_2$  steps, even though the same number of environment interactions are used in both cases.
4. Lastly, we prove an asymptotic guarantee on the quality of the solution found by our approach, compared to the best possible shaped-subgoal design.

The rest of the paper is organized as follows. Section 2 provides a literature review of related work. In Section 3, we introduce the details of the problem along with its mathematical model.

The proposed algorithm is given and discussed in Section 4. In Section 5, we conduct numerical experiments to show the effectiveness of the approach.

## 2 Related Work

RL has recently been tremendously successful in complex sequential decision-making problems, with applications in games (Mnih et al., 2013; Silver et al., 2017), robotics (Rusu et al., 2016; Mordatch et al., 2016; Hanna and Stone, 2017), healthcare (Moodie et al., 2012; Prasad et al., 2017) and many other areas (Yu et al., 2015; Bojarski et al., 2016). State-of-art algorithms (e.g. Grondman et al. (2012); Mnih et al. (2013); Guo et al. (2014)) inherently require a large number of observations from the environment and converge slowly in complex problems. Moreover, the problem of exploration in unknown environments continues to pose a challenge for many RL algorithms (Osband et al., 2013, 2014, 2016; Fortunato et al., 2017).

Naive exploration strategies such as  $\epsilon$ -greedy can lead to exponentially large data requirements. Many algorithms employ optimism approaches (Kearns and Singh, 2002; Stadie et al., 2015; Bellemare et al., 2016; Tang et al., 2017) and value-related methods (Osband et al., 2014; Russo and Van Roy, 2014; Morere and Ramos, 2018) to guide exploration. In the optimism approaches, Tang et al. (2017) assign an optimistic bonus to poorly-understood states and actions. Bellemare et al. (2016); Ostrovski et al. (2017) parametrize density estimates for state visits and utilize pseudo-counts. Stadie et al. (2015); Oh et al. (2015) learn the dynamics and choose action that leads to states that are poorly-explored or most dissimilar to recent states. Russo and Van Roy (2014); Osband and Van Roy (2017) focus on posterior sampling. In the value-related methods, Osband et al. (2014, 2017) leverage values by randomizing value functions. Osband et al. (2016) models the  $Q$ -value distribution via the bootstrap. Morere and Ramos (2018) use the uncertainty of  $Q$  values to direct exploration. Fortunato et al. (2017) adds parametric noise to the weights of neural networks.

The implementation of *intrinsic reward* (also called *intrinsic motivation*) is inspired by the response of dopamine neurons to sensory stimuli (Schultz, 1998; Redgrave and Gurney, 2006), and by psychology research (Harlow, 1950; Harter, 1981). Intrinsic reward helps robots learn increasingly complex behavior in a self-motivated way. There are many different sources of intrinsic reward,

including novelty (Huang and Weng, 2002), learning progress (Kaplan and Oudeyer, 2004), curiosity (Pathak et al., 2017; Burda et al., 2018), and surprise (Achiam and Sastry, 2017). Sorg et al. (2010); Guo et al. (2016) treat the intrinsic reward as parameters that influence the outcome of the planning process and train it via gradient ascent. Sorg et al. (2011) uses intrinsic reward as an alternative to the leaf-evaluation heuristic approach and extends Policy Gradient for Reward Design (PGRD) to learn the optimal reward. Zheng et al. (2018) designs an algorithm to learn the intrinsic rewards for policy-gradient based learning agents. Potential-based reward shaping (PBRS) (Ng et al., 1999) provides a way to modify the reward function that simultaneously maintains the optimal policy and potentially accelerates learning. PBRS has been used in a wide range of areas, including driving a bicycle (Randløv and Alstrøm, 1998), robotic training (Tenorio-Gonzalez et al., 2010), and video game artificial intelligence (Lample and Chaplot, 2017; Jiang et al., 2018). The agent’s performance is highly dependent on an informative reward signal (Ng et al., 1999); however, manual reward shaping can be a labor-intensive process that often requires a deep domain expertise.

To overcome the variation of the environment in real-world application, RL researchers are recently interested in leveraging the experience accumulated from previous tasks to improve the agent’s performance in a new task, including continual learning, transfer learning and meta learning. The idea has been realized by hierarchically learning from an easy task to a complicated task (Ring, 1994), learning the relationship among the MDPs (Wilson et al., 2007), initializing the parameters of the new task by using the information from previous tasks (Tanaka and Yamamura, 1997; Konidaris and Barto, 2006), probabilistic policy reuse (Fernández and Veloso, 2013), learning a parametrized policy that generalizes across tasks (Deisenroth et al., 2014), hierarchically structured policies (Frans et al., 2017), multi-task policy gradient method (Ammar et al., 2014), utilizing goal-conditioned value function (Mankowitz et al., 2018), distinguishing the important parameters to previous tasks (Vuorio et al., 2018), and learning exploration strategies from prior experience by gradient-based method (Gupta et al., 2018). We specify that the main novel focus of our paper is the *sample-efficiency*; for example, we explicitly account for training cost by building a surrogate model of the entire training curve.

Our approach of designing subgoals follows the Bayesian optimization (BO) paradigm that has recently emerged as powerful technique for the optimization of black-box functions, in particular for tuning ML models and design of experiments (Brochu et al., 2010; Snoek et al., 2012; Herbol

et al., 2018; Frazier, 2018). BO has recently been shown to be effective for optimizing in high-dimensional spaces (Hernández-Lobato et al., 2017; Wang et al., 2018; Nayebi et al., 2019). Our work bears resemblance and generalizes methods for network architecture search and optimization with multiple information sources (Swersky et al., 2013, 2014; Feurer et al., 2015; Domhan et al., 2015; Li et al., 2017; Klein et al., 2016; Poloczek et al., 2017). Their work differs in that they may observe directly the whole curve of the loss during training, whereas our setting only allows to observe the score of the policy after the underlying exploration process has completed (as motivated by the real-world applications described above).

### 3 Problem Formulation

Let  $\xi \in \Xi$  be a random variable that parameterizes the set of possible environments. Each environment is modeled by an MDP denoted by the tuple  $\langle \mathcal{S}, \mathcal{A}, g_\xi, R_\xi, \gamma \rangle$ , where  $\mathcal{S}$  and  $\mathcal{A}$  are the state and action spaces,  $g_\xi : \mathcal{S} \times \mathcal{A} \times \mathcal{W} \rightarrow \mathcal{S}$  is a transition function,  $\mathcal{W}$  is the outcome space associated with a noise distribution  $w$ ,  $R_\xi : \mathcal{S} \times \mathcal{A} \times \mathcal{S} \rightarrow \mathbb{R}$  is the reward function and  $\gamma \in (0, 1)$  is the discount factor. Our model assumes common state and action spaces across the distribution of MDPs (i.e., independent of  $\xi$ ), while the reward and transition functions vary with  $\xi$ . Given  $\mathcal{S}$  and  $\mathcal{A}$ , a *policy* is a mapping such that  $\pi(\cdot | s)$  is a distribution over  $\mathcal{A}$  for any state  $s \in \mathcal{S}$ . For any MDP  $\langle \mathcal{S}, \mathcal{A}, g_\xi, R_\xi, \gamma \rangle$ , define the *value function* of policy  $\pi$  at any state  $s$  as

$$V_\xi^\pi(s) = \mathbf{E}[\sum_{t=1}^{\infty} \gamma^{t-1} R_\xi(s_t, a_t, s_{t+1}) | \pi, s], \quad (1)$$

where  $s$  is the initial state,  $a_t \sim \pi(\cdot | s_t)$ , and  $\mathbf{E}$  is over noise  $w$  and stochastic policy  $\pi$ . The optimal value and policy is  $V_\xi^*(s) = \sup_\pi V_\xi^\pi(s)$  and  $\pi_\xi^*(s) \in \arg \max_{a \in \mathcal{A}} \mathbf{E}[R_\xi(s, a, s') + \gamma V_\xi^*(s') | s, a]$ .

We allow for  $\Xi$  to be an arbitrary set, so our model handles the case where there are an infinite number of possible environments. We also do not make any assumptions on the distribution of  $\xi$ , and in particular it is not assumed to be known. We refer to the sequence of training environments encountered by the agent simply by the realizations of the parameter  $\xi$ , denoted by  $\xi^1, \xi^2, \dots, \xi^N$ , where  $N$  is the total number of practice opportunities given to the agent.

### 3.1 Subgoals with Intrinsic Reward Shaping

The reward function  $R_\xi$  is called the *extrinsic reward* given to the agent by the environment — this is the quantity that we aim to maximize in a cumulative fashion. However, it is often the case that these rewards are sparse and delayed, and therefore produce little to no learning signal for the agent. For example, in the case of searching for a goal, most states are associated with zero reward, while only the goal state(s) contain positive reward. For this reason, the agent essentially must perform random exploration and does not start learning until the first time it wanders to the goal. The time it takes to find the goal under a random exploration strategy, such as  $\epsilon$ -greedy, could be prohibitively long.

We propose to use subgoals with intrinsic reward shaping (details below) to provide an artificial reward signal for the agent, that if properly designed, can direct the agent to explore useful parts of the state space. In other words, it is difficult to learn an optimal policy  $\pi_\xi^*$  using a small number of interactions; instead, we aim to learn another policy, augmented by intrinsic subgoals and rewards, that can achieve performance similar to  $V_\xi^*$ . To illustrate, consider a distribution of maze environments, where the location of a door is uncertain but likely to be on the right half of the room; here, a useful subgoal would be to move the agent towards the right so that it is likely to be in the vicinity of the door across many different realizations of the environment  $\xi$ . This makes it easier for the RL algorithm and its simple exploration policy (e.g.,  $\epsilon$ -greedy) to discover the precise location of the door.

Let  $k$  be the number of subgoals and  $\theta \in \Theta$  represent a parameterization. Then, a subgoal design can be described via

$$(\{\mathcal{S}_{\theta_1}, \mathcal{S}_{\theta_2}, \dots, \mathcal{S}_{\theta_k}\}, \{R_{\theta_1}, R_{\theta_2}, \dots, R_{\theta_k}\}), \tag{2}$$

where for  $j = 1, 2, \dots, k$ ,  $\mathcal{S}_{\theta_j} \subseteq \mathcal{S}$  is a subset of the state space representing the states associated with subgoal  $j$  (i.e., if the agent lands in some state in  $\mathcal{S}_{\theta_j}$ , then subgoal  $j$  is considered “completed”).  $R_{\theta_j}$  is a *potential-based reward shaping function* for subgoal  $j$ ; see [Ng et al. \(1999\)](#) for additional details regarding PBRS, which we have adapted for the subgoal case. Concretely,  $R_{\theta_j}(s, s') = \gamma\Phi_{\theta_j}(s') - \Phi_{\theta_j}(s)$ , where  $\Phi_{\theta_j}$  is a potential function over  $\mathcal{S}$  such that states in  $\mathcal{S}_{\theta_j}$  have the highest

potential. This means that the change in potential motivates the agent to move towards subgoal  $j$ .

Each choice of shaped subgoals  $\theta$  introduces an auxiliary state  $i \in \mathcal{I}_k := \{0, 1, \dots, k\}$ , where  $i$  simply represents the number of subgoals reached by the agent so far. Initially, we have  $i_0 = 0$ . The state of the new system is  $(s, i) \in \mathcal{S} \times \mathcal{I}_k$  and the transitions are  $s' = g_\xi(s, a, w)$  and

$$i' = i + \mathbf{1}_{\{s' \in \mathcal{S}_{i+1}\}} =: h_\theta(s, a, w, i),$$

where we take  $\mathcal{S}_{k+1} = \emptyset$ . This means the auxiliary state  $i$  is updated to  $i + 1$  whenever  $s'$  reaches the next subgoal. When the auxiliary state is  $i$ , the only intrinsic reward is  $R_{\theta, i+1}(s, s')$ , and we take  $R_{\theta, k+1} \equiv 0$  (i.e., there is no additional intrinsic reward after reaching the  $k$ th subgoal). Intuitively, we can imagine that a different shaped intrinsic reward function appears as we complete each subgoal; this reward function directs the agent toward the next subgoal. Let  $R_\theta(s, i, s') = R_{\theta, i+1}(s, s')$  denote the additional intrinsic reward supplemented to the agent by subgoal parameter  $\theta$ . Our *augmented* MDP has reward function

$$R_{\xi, \theta}(s, i, a, s') = R_\xi(s, a, s') + R_\theta(s, i, s'),$$

and we define the value function for the new MDP as

$$V_{\xi, \theta}^\pi(s, i) = \mathbf{E}[\sum_{t=1}^{\infty} \gamma^{t-1} R_{\xi, \theta}(s_t, i_t, a_t, s_{t+1}) \mid \pi, s, i], \quad (3)$$

where, with a slight abuse/reuse of notation,  $\pi$  is a policy acting on the new state space  $\mathcal{S} \times \mathcal{I}_\theta$ .

To illustrate how the subgoals work, we consider a domain as in Figure 1a. It is a  $10 \times 10$  gridworld with a wall (the gray area) and a closed door (at the right-hand-side of the wall). The agent starts from the lower-left blue-shaded grid and may in each step choose an action from the action space consisting of the four compass directions. The goal is to reach the upper left red-shaded squares to collect a reward of one. To move through the door, a key with size  $2 \times 2$  located in the light yellow area must be collected by the agent. A subgoal design example with  $k = 3$  is shown in Figure 1b, where the circle, the triangle, and the cross represent the first, the second, and the third subgoal respectively. The initial auxiliary state is  $i = 0$ , and the only intrinsic reward is provided by the circle subgoal (Figure 1c). The form of the intrinsic reward,  $R_{\theta_j}(s, s') = \gamma \Phi_{\theta_j}(s') - \Phi_{\theta_j}(s)$ ,



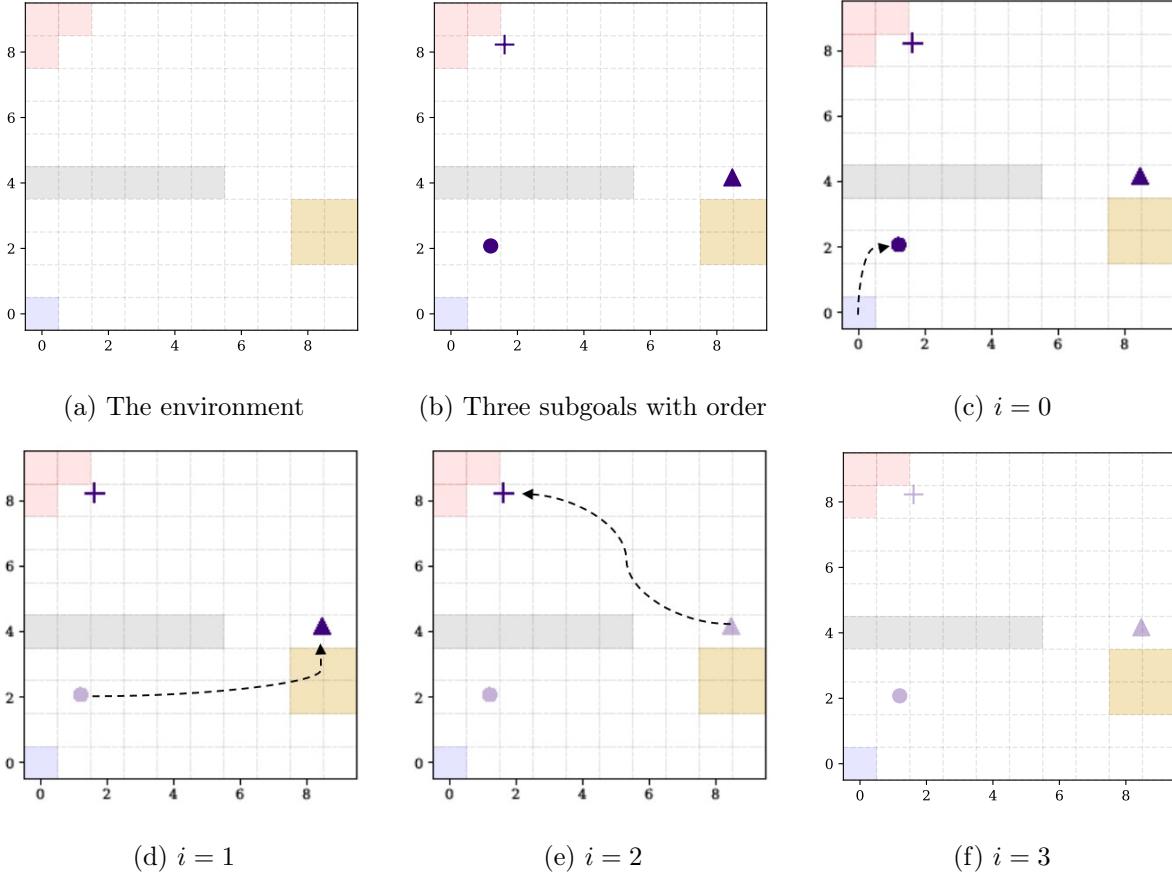


Figure 1: The mechanism of subgoals with intrinsic reward shaping

makes the circle subgoal attractive to the agent. When the circle subgoal is collected by the agent, the auxiliary state becomes  $i = 1$ , and the only intrinsic reward is provided by the triangle (Figure 1d). The agent then collects the triangle subgoal (Figure 1e), and similarly collects the cross subgoal (Figure 1f).

Roughly speaking, our goal is to find a set of parameters  $\theta$  that can incentivize the agent to intelligently explore environments drawn from the distribution of  $\xi$ . The hope is that at test time, the agent is able to quickly learn a good policy after observing only a small number of samples from the test environment.

### 3.2 Optimizing Subgoals for Exploration

The problem of selecting subgoals depends on the agent’s learning algorithm, which could in principle be any RL algorithm. In the numerical results of Section 5, our agent learns via  $Q$ -learning (Watkins

and Dayan, 1992). However, for the time being, we do not place any restrictions on the RL algorithm (besides assuming that it is fixed throughout the training and test environments) and simply define  $\pi_{\xi, \theta}^{\tau}$  to be the policy, with state space  $\mathcal{S} \times \mathcal{I}_{\theta}$ , attained after the agent learns for  $\tau$  interactions in environment  $\xi$  augmented by shaped subgoals  $\theta$ . Thus, the RL algorithm is optimizing the objective  $V_{\xi, \theta}^{\pi}$ , as defined in (3). Note that  $\pi_{\xi, \theta}^{\tau}$  is in general a random quantity depending on both the interactions with the environment and any inherent stochasticity in the learning algorithm (e.g., the original  $\epsilon$ -greedy exploration used in  $Q$ -learning).

However, our original objective  $V_{\xi}^{\pi}$  does not include the subgoal rewards. To bridge the gap, we define

$$\tilde{V}_{\xi}(\pi) = \mathbf{E}[\sum_{t=1}^{\infty} \gamma^{t-1} R_{\xi}(s_t, a_t, s_{t+1}) | \pi], \quad (4)$$

as the value function associated with an augmented policy  $\pi(\cdot | s, i)$  that only incurs extrinsic rewards. Let  $\tau_{\max}$  be the number of interactions available in test environment. Combining all of the pieces, we have the following optimization problem  $\max_{\theta \in \Theta} u(\theta, \tau_{\max})$ , where  $u(\theta, \tau) := \mathbf{E}[\tilde{V}_{\xi}(\pi_{\xi, \theta}^{\tau})]$ . Here the expectation is taken over the environment  $\xi$  and the stochasticity of the learning algorithm  $\pi_{\xi, \theta}^{\tau}$ . The interpretation of the objective is: we are looking for a subgoal design  $\theta$  that incentivizes the agent to explore random environments  $\xi$  in a way that maximizes the expected performance of a policy learned by the fixed RL algorithm in  $\tau_{\max}$  interactions. Finally, to reduce the variance of performance observations, we may average the observed cumulative reward over  $q$  i.i.d. replications ( $1 \leq q \leq q_{\max}$ ), for a total of  $\tau_{\max} \cdot q$  interactions.

### 3.3 The Sequential Optimization Setup

As discussed previously, we do not assume the ability to compute the expectation in  $\mathbf{E}[\tilde{V}_{\xi}(\pi_{\xi, \theta}^{\tau})]$  and can only observe the performance of policies in a sequence of environment realizations  $\xi^1, \xi^2, \dots, \xi^N$ . Let us now move on to discuss the costly training aspect of the model, where every interaction with training environments incurs a cost, e.g., time, labor, or equipment. Therefore, three decisions are made at the beginning of training opportunity  $n \in \{1, 2, \dots, N\}$ : a choice of subgoal design  $\theta^n$ , the maximum episode length  $\tau^n$ , and the number  $q^n$  of training episodes to use for this particular  $\theta^n$ . Thus, the agent interacts  $\tau^n q^n$  times with the environments. The idea is that the performance of the policy trained using shorter episode than  $\tau_{\max}$  could be informative of the performance of the

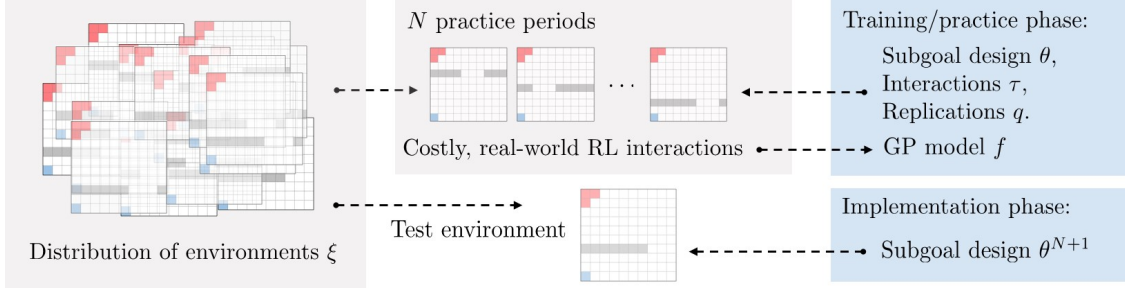


Figure 2: Outline of the BESD algorithm

policy trained for  $\tau_{\max}$  steps, and fewer replications than  $q_{\max}$  could provide a good estimation to the performance of the policy.

Let  $\mathcal{T}$  and  $\mathcal{Q}$  be the set of possible values of  $\tau$  and  $q$  respectively under consideration, and let  $\mathcal{Z} = \Theta \times \mathcal{T} \times \mathcal{Q}$  be the decision space. We then observe  $y^n = u(\theta^n, \tau^n) + \varepsilon^n(q^n)$  in each episode, where  $\varepsilon^n$  is a standard normal random variable that captures the sampling noise due to  $\xi^n$ , the noise in  $\pi_{\xi, \theta^n}^{\tau^n}$  due to a sample run of the RL algorithm, and the evaluation noise due to an inability to exactly compute  $\tilde{V}_{\xi}$  (even when the environment  $\xi$  is fixed). Note that the observations of the  $q^n$  replications are averaged in iteration  $n$ , thereby reducing the observational noise  $\varepsilon^n(q^n)$ . After training opportunity  $N$ , we reach the *implementation phase* and output a subgoal design  $\theta^{N+1}$  that is used on the test MDP  $\xi^{N+1}$  with an agent that has a budget of  $\tau_{\max}$  interactions in each episode to spend in the test environment. The cost incurred is the total number of interactions used in training:  $\sum_{n=1}^N \tau^n q^n$ .

## 4 The BESD Algorithm

Our Bayesian approach for designing subgoals consists of two components: a tailored probabilistic model and an algorithm for selecting the next subgoal and interaction budget to observe. The budget is split between the number of steps that the underlying RL policy is run (more may increase the chance of collecting a reward) and the number of replications (more reduce the observational noise). We call the overall approach *Bayesian exploratory subgoal design* (BESD). For the remainder of the paper, through a slight abuse of notation, we assume that the subgoal design parameter  $\theta$  described in (2) can be written as a vector in  $\mathbb{R}^d$ .

## 4.1 The Model

We want to learn the value of subgoals for a “typical” MDP sampled from the unknown distribution of  $\xi$ . We model the expected performance of the underlying RL policy when executed with subgoals  $\theta$  for  $\tau \in \mathbb{N}$  interactions by the latent function  $u$ . The expectation is taken over  $\xi$  and the randomness introduced by the underlying policy. We suppose observations  $y(\theta, \tau) \sim \mathcal{N}(g(\theta, \tau), \lambda(\theta, \tau))$  when evaluating subgoals  $\theta$  for  $\tau$  steps, where  $\lambda$  gives the variance in the observations due to the randomness in  $\xi$  and the underlying policy. Note that these observations are i.i.d., since a new MDP is sampled in each iteration. We suppose that the function  $\lambda$  is finite and known, although in practice it is learned from data, e.g., via a maximum likelihood estimate (MLE) or via Gaussian process (GP) regression.

We propose a generative model that gives a GP prior  $f$  on the latent function  $u$  with mean function  $\mu : \Theta \times \mathcal{T} \rightarrow \mathbb{R}$  and covariance function  $k : \mathcal{Z} \times \mathcal{Z} \rightarrow \mathbb{R}_+$ . More precisely, we set  $\mu$  to the mean of an initial set of samples and use a multidimensional product kernel  $k((\theta, \tau), (\theta', \tau')) = k_\theta(\theta, \theta') k_\tau(\tau, \tau')$ . The kernel  $k_\theta$  is the (5/2)-Matérn kernel and  $k_\tau(\tau, \tau')$  is a polynomial kernel  $k_\tau(\tau, \tau') = \phi(\tau)^\top \Sigma_\phi \phi(\tau')$  with  $\phi(\tau) = (1, \tau)^\top$  and hyperparameters  $\Sigma_\phi$ . We observe that the covariance under  $k$  is large only if the covariance is large under both  $k_\theta$  and  $k_\tau$ . Note that kernels are closed under multiplication, and since we have a GP prior and a Gaussian sampling distribution, we may use standard GP machinery to analytically compute the posterior distribution conditioned on the history after  $n$  steps:

$$H^n = (\theta^1, \tau^1, q^1, y^1, \theta^2, \tau^2, q^2, y^2, \dots, \theta^n, \tau^n, q^n, y^n).$$

See [Rasmussen and Williams \(2006, Ch. 2.2\)](#) for details.

## 4.2 Bayesian Exploratory Subgoal Design

Suppose the training budget is used up after  $N$  steps. Then the optimal risk-neutral decision is to use subgoals on the test MDP  $\xi^{N+1}$  that have maximum expected score under the posterior. The expected score of this choice is  $\mu_N^*$  where

$$\mu_n^* := \max_{\theta'} \mu^n(\theta', \tau_{\max}),$$

and  $\mu^n(\theta, \tau) = \mathbf{E}_n[f(\theta, \tau)]$ . Here  $\mathbf{E}_n$  is the conditional expectation with respect to the history  $H^n$ . Note that although we are allowed to use fewer than  $\tau_{\max}$  interactions and  $q_{\max}$  replications in training environments to reduce cost, we suppose that the agent uses its full budget for the test MDP. The proposed algorithm proceeds in iterations, designating one set of subgoals  $\theta$  to be evaluated in each iteration. Thus, we take a myopic approach, i.e., we suppose that this is the last training MDP before the test MDP. If we evaluate the subgoals  $\theta$  next for  $\tau$  steps and  $q$  replications, then the *expected gain in score* (GiS) on the test MDP is

$$\text{GiS}^n(\theta, \tau, q) = \mathbf{E}_n[\mu_{n+1}^* \mid \theta^{n+1} = \theta, \tau^{n+1} = \tau, q^{n+1} = q] - \mu_n^*.$$

Therefore, the one-step optimal strategy is to choose the next subgoals  $\theta^{n+1}$ , interaction  $\tau^{n+1}$ , and replication  $q^{n+1}$  so that  $\text{GiS}^n$  is maximized. However, this strategy would generally allocate a maximum number of steps  $\tau_{\max}$  and replications  $q_{\max}$  for the evaluation of the next subgoal design, as observing  $\tau_{\max}$  during training is most informative of the test conditions, and repeating for  $q_{\max}$  replications reduces the noise maximally to  $\lambda(\theta, \tau_{\max})/q_{\max}$  (where the agent will exhaust the entire budget). In other words, this strategy does not consider the cost of training. Hence, we propose an acquisition function that maximizes the *gain in score per effort* by dividing the GiS function by the budget ( $q^{n+1} \cdot \tau^{n+1}$ ), resulting in an algorithm that selects

$$(\theta^{n+1}, \tau^{n+1}, q^{n+1}) \in \arg \max_{\theta, \tau, q} \frac{\text{GiS}^n(\theta, \tau, q)}{q\tau}. \quad (5)$$

In settings with other factors that influence the cost of training (e.g., an overhead for creating new training environments), we may adjust the denominator accordingly. To make this optimization problem tractable, we first replace the search domain  $\Theta$  in (5) by a discrete set  $\Theta' \subseteq \Theta$ , for example selected by a Latin Hypercube design. We may then compute  $\text{GiS}^n(\theta, \tau, q)/(q\tau)$  exactly: In Appendix E, we detail how to find a maximizer  $(\theta^{n+1}, \tau^{n+1}, q^{n+1})$  efficiently. An outline of BESD is summarized in Figure 2. Note that by construction BESD is Bayes optimal (per unit cost) for the last step, in expectation.

**Proposition 1.** *BESD achieves an optimal expected information gain per unit cost (with respect to  $\Theta'$ ) for the case of  $N = 1$ .*

In Theorem 2, we provide an additive bound on the difference between the solution of BESD and the unknown optimum, as the number of iterations  $N \rightarrow \infty$ . For convenience, we suppose  $\mu(\theta, \tau) = 0$  for all  $\theta, \tau$ , and  $\Sigma$  is at least four times differentiable. Define  $\theta^{\text{OPT}} \in \arg \max_{\theta' \in \Theta} f(\theta', \tau_{\max})$  and  $d = \max_{\theta' \in \Theta} \min_{\theta'' \in \Theta'} \text{dist}(\theta', \theta'')$ . Define  $\bar{\theta} \in \Theta'$  as  $\text{dist}(\bar{\theta}, \theta^{\text{OPT}}) \leq d$ . Theorem 1 states the relationship between  $f(\theta_N^*, \tau_{\max})$  and  $f(\bar{\theta}, \tau_{\max})$  as the number of iterations  $N \rightarrow \infty$ . Its proof is given in Appendix A.

**Theorem 1.** *As  $N \rightarrow \infty$ ,  $\lim f(\theta_N^*, \tau_{\max}) \geq f(\bar{\theta}, \tau_{\max})$  almost surely.*

**Theorem 2.** *Let  $\theta_N^* \in \Theta'$  be the point that BESD recommends in iteration  $N$ . For each  $p \in [0, 1)$ , there is a constant  $K_p$  such that with probability  $p$*

$$\lim_{N \rightarrow \infty} f(\theta_N^*, \tau_{\max}) \geq f(\theta^{\text{OPT}}, \tau_{\max}) - K_p \cdot d.$$

*Proof.* Recall that  $N$  is the number of training opportunities. We establish an additive bound on the loss of the solution obtained by the algorithm with respect to the unknown optimum, as the number of queries  $N \rightarrow \infty$ . Recall that we suppose  $\mu(\theta, \tau) = 0$  for all  $\theta, \tau$ , and  $\Sigma$  is at least four times differentiable. Suppose  $f \sim \text{GP}(\mu, \Sigma)$ . Then the sample  $f(\cdot, \tau_{\max})$  from the distribution over functions is itself twice continuously differentiable with probability one. Therefore, the extrema of  $\frac{\partial}{\partial \theta_i} f(\theta, \tau_{\max})$  over  $\Theta$  are bounded. Specifically, since the partial derivatives of  $\text{GP}(\mu, \Sigma)$  with respect  $\theta_i$  are also GPs for our choice, we can compute for every  $p \in [0, 1)$  a constant  $K_p$  such that  $f(\cdot, \tau_{\max})$  is  $K_p$ -Lipschitz continuous on  $\Theta$ , i.e.,  $|f(\theta_1, \tau_{\max}) - f(\theta_2, \tau_{\max})| \leq K_p |\theta_1 - \theta_2|$ , with probability at least  $p$ . Then there is an  $\bar{\theta} \in \Theta'$  with  $\text{dist}(\bar{\theta}, \theta^{\text{OPT}}) \leq d$ , and hence

$$f(\theta^{\text{OPT}}, \tau_{\max}) - f(\bar{\theta}, \tau_{\max}) \leq K_p \cdot d. \tag{6}$$

Theorem 1 completes the proof of Theorem 2 since (6) holds with probability  $p$ . □

## 5 Numerical Experiments

We evaluate the performance of BESD and several other baseline algorithms on a number of domains. We compare against standard  $Q$ -learning (QL) (Watkins, 1989), “transfer”  $Q$ -learning (TQL),

---

**Algorithm 1:** Bayesian Exploratory Subgoal Design

---

**Input:** Estimate hyperparameters of the GP prior using initial samples.

**Output:** A subgoal recommendation  $\theta^{N+1}$  that maximizes  $\mu^N(\theta, \tau_{\max})$

- 1 **for**  $n = 0, 1, \dots, N$  **do**
  - 2     Compute next decision  $(\theta^{n+1}, \tau^{n+1}, q^{n+1})$  according to the acquisition function (5).
  - 3     Train in environment  $\xi^{n+1}$  according to (3) using  $(\theta^{n+1}, \tau^{n+1}, q^{n+1})$ . Observe  $y^{n+1}$ .
  - 4     Update the posterior distribution with the new data  $\{(\theta^{n+1}, \tau^{n+1}, q^{n+1}), y^{n+1}\}$  and increment counter  $n$ .
  - 5 **end**
- 

Hyperband (HB) (Li et al., 2017), the expected improvement algorithm (EI) (Moćkus, 1975; Jones et al., 1998), and the lower confidence bound algorithm (LCB) (Cox and John, 1992). Our proposed technique, BESD, is given two choices for the replications (unless stated otherwise,  $\mathcal{Q} = \{5, 20\}$ ) and three choices for the length of the episode in each replication:  $\mathcal{T} = \{\tau_{\min}, \tau_{\text{mid}}, \tau_{\max}\}$ , where the values vary across the different problem domains and are reported below. The first baseline is the QL algorithm of Watkins (1989) with no subgoals or reward shaping: that is, we directly run QL on environment  $\xi^{N+1}$  for  $\tau_{\max}$  interactions. Details about the other algorithms are given in Appendix B.

We report the mean performance of the best subgoal design found by an algorithm as a function of the total training cost that has been utilized so far. The error bars indicate  $\pm 2$  standard errors of the mean. Specifically, to assess the performance of an algorithm after  $i$  steps, we take its recommendation after that steps and test it on a sample of MDPs from the distribution group. BESD was implemented in Python 2.7 using the MOE package (Clark et al., 2014) and will be open-sourced upon acceptance of the manuscript. The observational noise  $\lambda$  was set to a maximum likelihood estimate for the smallest value of  $q$ , although a more sophisticated approach like Gaussian process regression might improve the performance of BESD even further. The initial data size is ten for each value of  $\tau$ . We use either two or three subgoals in all experiments. The potential function at state  $(s, j)$  is  $\Phi_j(s) = w_1 \exp[(s-j)^2/w_2]$ . Unless stated otherwise,  $w_1 = 0.2$ ,  $w_2 = 10$  in the experiments.

**Gridworlds with Walls.** The first domain is a distribution of  $10 \times 10$  gridworlds (GW10), where the goal is to reach the upper left square that is shaded red in Figure 3a to collect a reward of one. The agent starts from the lower-left grid square shaded in blue and may in each step

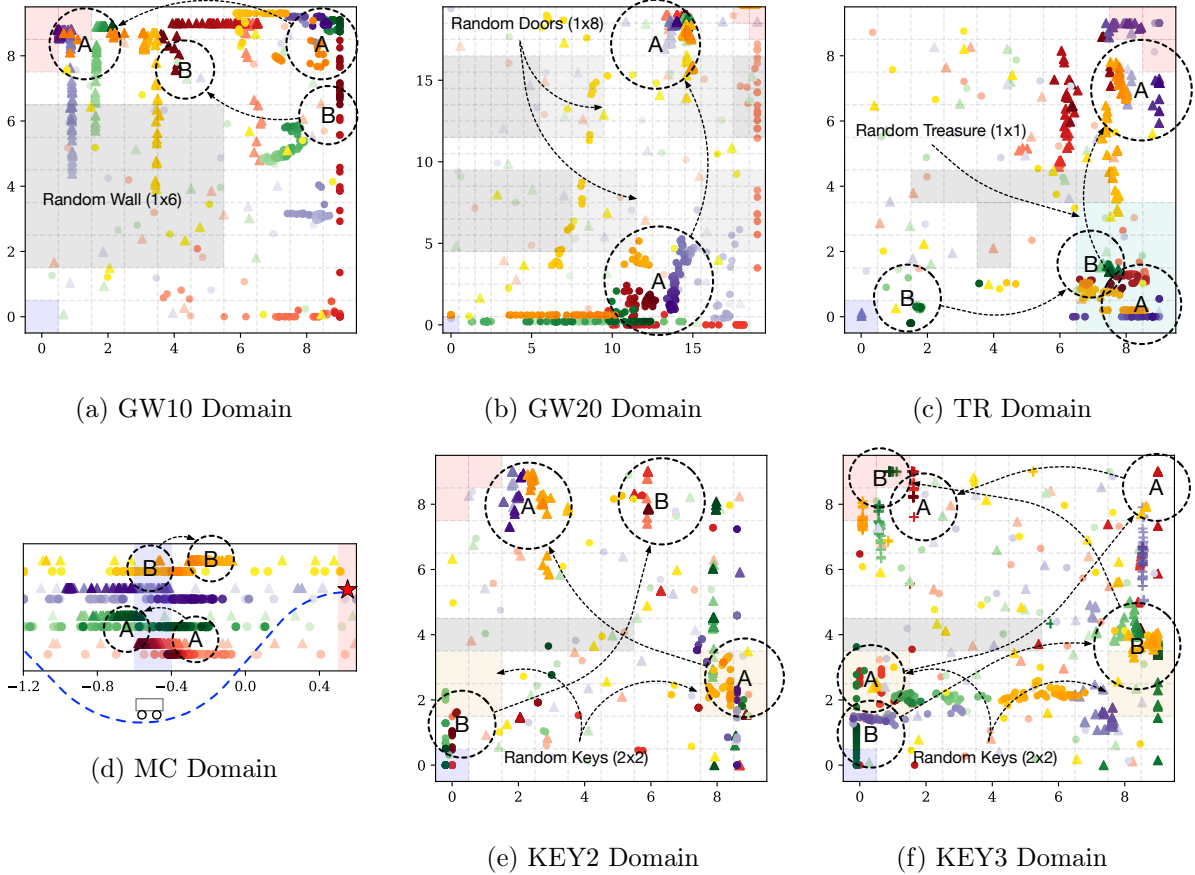


Figure 3: Recommendation paths

choose an action from the action space consisting of the four compass directions. Each gridworld is partitioned by a wall into two rooms. The wall, randomly located in one of the middle five rows in the gridworld, has a door located on four grid squares on its right. The agent will stay in the current location when it hits the wall. There is a small amount of “wind” or noise in the transition: the agent moves in a random direction with a probability that is itself uniformly distributed between 0 and 0.02 (thus,  $\xi$  determines the wall location and the wind probability). We use  $\mathcal{T} = \{200, 600, 1000\}$ . Subgoal locations are limited to the continuous subset of  $\mathbb{R}^2$  which contains the grid, e.g.  $\Theta = ([0, 10] \times [0, 10])^2$  for GW10. Let  $\theta_i^{*,n}$  be the subgoal recommendation in iteration  $n$  of algorithm  $i \in \{\text{BESD, HB, EI, LCB}\}$ . For the latter three baselines, we let  $\theta_i^{*,n}$  be the subgoal with the highest score up until iteration  $n$ . Note that this makes their performance only look stronger! Figure 3a displays four realizations of the initial data and the “recommendation paths” of BESD, defined as  $(\theta_{\text{BESD}}^{*1}, \theta_{\text{BESD}}^{*2}, \dots, \theta_{\text{BESD}}^{*n})$  for the GW10 domain. Each color corresponds to



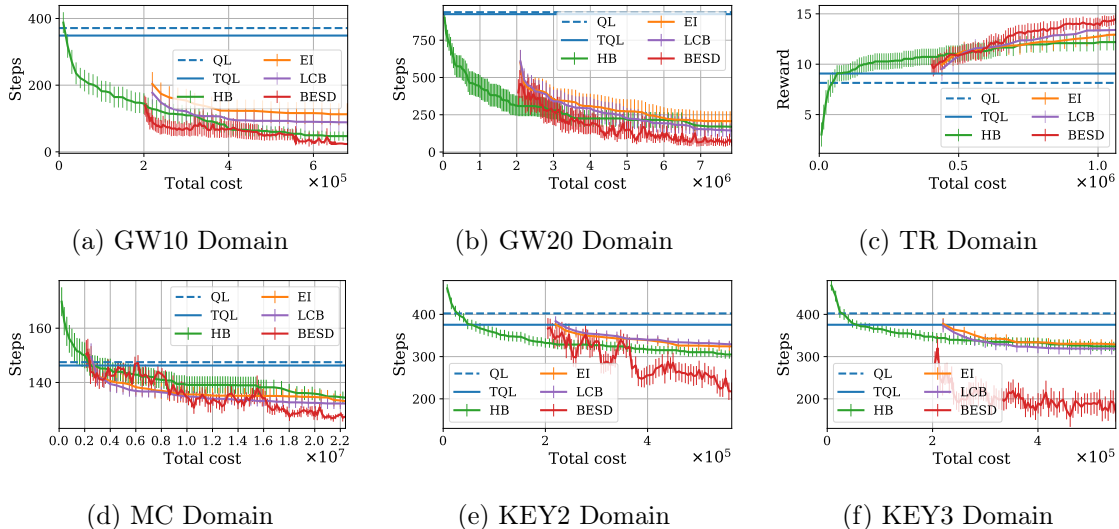


Figure 4: Performance as a function of the experimentation costs

one realization, and the color becomes deeper as  $n$  increases, with the most light points being the initial samples. The circles and triangles represent the first and second subgoals respectively. The possible locations of the random wall are shaded in gray.

We point out two “subgoal-sets of interest” using ‘A’ and ‘B’ labels, which are commonly recommended sets of subgoals in later iterations of BESD (darker circle and triangle pairs). Generally speaking, the first subgoal “path” moves toward the upper right corner, which motivates the agent to bypass the random wall. The second subgoal has a trend toward the upper left corner, directing the agent towards the goal after bypassing the wall. Note that the agent itself follows the standard RL paradigm and does not have any knowledge about the model of the gridworld.

**Three-Room Gridworlds.** The last domain is a distribution of  $20 \times 20$  gridworlds with three rooms separated by two walls (GW20). As shown in Figure 3b, the walls are randomly located in the middle rows (dark gray). A door of size 8 is randomly located somewhere within the wall, shaded in light gray. The noise due to wind is the same as in GW10. Let  $\mathcal{Q} = \{20\}$  and  $\mathcal{T} = \{4000, 7000, 10000\}$ . Recommendation paths are shown in Figure 3b. As more environments are observed, the first subgoal moves downward, toward the entrance of the first door. The second subgoal converges toward the exit of the second door, moving the agent near the goal. A successful path induced by a subgoal pair in the circles labeled ‘A’ is shaped like a reverse ‘Z’.

**Treasure-in-Room Gridworlds.** The second domain (TR) is a  $10 \times 10$  gridworld with a

“treasure” in a small room; see Figure 3c. The light green area shows the possible positions of the treasure. The agent gets a reward 10 upon entering the square with treasure, and a reward 10 upon reaching the goal. The cumulative reward, however, is zero if the agent does not find the goal within the budget. The discount factor  $\gamma = 0.98$  for the reported results and  $\mathcal{T} = \{400, 1200, 2000\}$ . Subgoal-pair ‘B’ is often recommended in earlier iterations of **BESD** (which leads directly to the “treasure”), but later on, **BESD** discovers the room and recommends pair ‘A’.

**The Mountain-car Problem.** The mountain-car domain (MC) is the standard RL benchmark environment; see, e.g., Sutton and Barto (2018). The start point is randomly located in  $[-0.6, -0.4]$ , and the replication and interaction sets are  $\mathcal{Q} = \{10, 50\}$  and  $\mathcal{T} = \{4000, 7000, 10000\}$  respectively. The subgoal-pairs discovered by **BESD** are shown in Figure 3d; they tend to be on opposite sides of the agent’s starting location, thereby creating back-and-forth movement needed to generate momentum and move up the mountain.

**Key-Door Gridworlds.** In domains KEY2 (with two subgoals) and KEY3 (with three subgoals), we consider a  $10 \times 10$  gridworld with one wall and a “key” to open a closed door (at the right-hand-side of the wall), as shown in Figures 3e and 3f. A key with size  $2 \times 2$  is randomly located in the light yellow areas, which introduces much diversity to the environment, and  $\mathcal{T} = \{400, 700, 1000\}$ . As pointed out in Figure 3f, the two yellow areas are important for the agent to move through the door to the other room. The first subgoals converge to the yellow area near the start. The second subgoals converge to either the other yellow area or the area above in the upper room, leading the agent directly moving to the possible “key” area or motivating the agent to explore that area by the dense rewards. And the third subgoals converge to the goal. The labeled subgoal pairs clearly show that **BESD** has discovered an intelligent exploration strategy. The two subgoals in KEY2 domain emphasize one of the yellow areas, as shown in Figure 3e, incurring some probability for the agent to explore in the lower room to get the “key”.

Figures 4a-4d show the expected score in the test MDP of each algorithm as a function of the total cumulative cost. We note that **BESD** is able to learn even using small budgets (and indeed, it relies on these low-cost observations often); therefore, it is much cheaper than training with budget  $q_{\max}\tau_{\max}$ . The initial sample cost of **BESD** is the same as that of **EI** and **LCB** in our simulated environments, since we can get the observations of  $\tau_{\min}$ ,  $\tau_{\text{mid}}$ , and  $\tau_{\max}$  from a sample with  $\tau_{\max}$ . **BESD** outperforms **EI** and **LCB** significantly in the expected score. On the other hand, the initial

sample is expensive when compared to HB, making HB competitive in the easiest domain GW10. As the complexity of the environments grows, however, BESD quickly outperforms HB in the long run. We point out that Figures 4e and 4f show that two subgoals achieve better result than the baselines, and three subgoals perform even better, which demonstrates the benefit of expanding the dimension of the parameterization space. Table 1 in Appendix C provides evidence of the benefits brought by the recommendations generated by BESD.

## 6 Conclusion

Incentivizing exploration is a central challenge in applying RL in real-world settings, since interactions with the environment are typically limited or expensive. If available, simulations can provide larger numbers of interactions but introduce an unknown model error that one must cope with. We propose BESD, which is able to, in a sample-efficient manner, set subgoals with an intrinsic shaped reward that aids the agent in scenarios with sparse and delayed rewards, thereby reducing the number of interactions needed to obtain a good solution. Here we focus on the general setup where we train on a series of related tasks before the final evaluation on the test task. An experimental evaluation demonstrates that BESD achieves considerably better solutions than a comprehensive field of baseline methods on a variety of complex tasks. Moreover, recommendation paths show that BESD discovers solutions that induce interesting exploration strategies.

## References

- J. Achiam and S. Sastry. Surprise-based intrinsic motivation for deep reinforcement learning. *arXiv preprint arXiv:1703.01732*, 2017.
- H. B. Ammar, E. Eaton, P. Ruvolo, and M. Taylor. Online multi-task learning for policy gradient methods. In *International Conference on Machine Learning*, pages 1206–1214, 2014.
- D. S. Apostolopoulos, L. Pedersen, B. N. Shamah, K. Shillcutt, M. D. Wagner, and W. L. Whittaker. Robotic antarctic meteorite search: Outcomes. In *International Conference on Robotics and Automation*, volume 4, pages 4174–4179. IEEE, 2001.
- M. Bellemare, S. Srinivasan, G. Ostrovski, T. Schaul, D. Saxton, and R. Munos. Unifying count-based exploration and intrinsic motivation. In *Advances in Neural Information Processing Systems*, pages 1471–1479, 2016.
- M. Bojarski, D. Del Testa, D. Dworakowski, B. Firner, B. Flepp, P. Goyal, L. D. Jackel, M. Monfort, U. Muller, J. Zhang, et al. End to end learning for self-driving cars. *arXiv preprint arXiv:1604.07316*, 2016.
- E. Brochu, V. M. Cora, and N. De Freitas. A tutorial on Bayesian optimization of expensive cost functions, with application to active user modeling and hierarchical reinforcement learning. *arXiv preprint arXiv:1012.2599*, 2010.
- Y. Burda, H. Edwards, D. Pathak, A. Storkey, T. Darrell, and A. A. Efros. Large-scale study of curiosity-driven learning. *arXiv preprint arXiv:1808.04355*, 2018.
- S. Clark, E. Liu, P. Frazier, J. Wang, D. Oktay, and N. Vesdapunt. Moe: A global, black box optimization engine for real world metric optimization. <https://github.com/Yelp/MOE>, 2014.
- D. D. Cox and S. John. A statistical method for global optimization. In *International Conference on Systems, Man, and Cybernetics*, pages 1241–1246. IEEE, 1992.
- N. T. Dee, M. Bedewy, A. Rao, J. Beroz, B. Lee, E. R. Meshot, C. A. Chazot, P. R. Kidambi, H. Zhao, T. Serbowicz, et al. In situ mechanochemical modulation of carbon nanotube forest growth. *Chemistry of Materials*, 2018.
- M. P. Deisenroth, P. Englert, J. Peters, and D. Fox. Multi-task policy search for robotics. In *International Conference on Robotics and Automation*, 2014.

- T. Domhan, J. T. Springenberg, and F. Hutter. Speeding up automatic hyperparameter optimization of deep neural networks by extrapolation of learning curves. In *International Joint Conferences on Artificial Intelligence*, volume 15, pages 3460–8, 2015.
- D. Ferguson, A. Morris, D. Haehnel, C. Baker, Z. Omohundro, C. Reverte, S. Thayer, C. Whittaker, W. Whittaker, W. Burgard, et al. An autonomous robotic system for mapping abandoned mines. In *Advances in Neural Information Processing Systems*, pages 587–594, 2004.
- F. Fernández and M. Veloso. Learning domain structure through probabilistic policy reuse in reinforcement learning. In *Progress in Artificial Intelligence*, volume 2, pages 13–27. Springer, 2013.
- M. Feurer, J. T. Springenberg, and F. Hutter. Initializing Bayesian hyperparameter optimization via meta-learning. In *Association for the Advancement of Artificial Intelligence*, pages 1128–1135, 2015.
- M. Fortunato, M. G. Azar, B. Piot, J. Menick, I. Osband, A. Graves, V. Mnih, R. Munos, D. Hassabis, O. Pietquin, et al. Noisy networks for exploration. *arXiv preprint arXiv:1706.10295*, 2017.
- K. Frans, J. Ho, X. Chen, P. Abbeel, and J. Schulman. Meta learning shared hierarchies. *arXiv preprint arXiv:1710.09767*, 2017.
- P. Frazier, W. Powell, and S. Dayanik. The knowledge-gradient policy for correlated normal beliefs. *INFORMS Journal on Computing*, 21(4):599–613, 2009.
- P. I. Frazier. Bayesian optimization. In *Recent Advances in Optimization and Modeling of Contemporary Problems*, pages 255–278. INFORMS, 2018.
- J. González. GPyOpt: A Bayesian optimization framework in Python. <http://github.com/SheffieldML/GPyOpt>, 2016.
- I. Grondman, L. Busoniu, G. A. Lopes, and R. Babuska. A survey of actor-critic reinforcement learning: Standard and natural policy gradients. *Transactions on Systems, Man, and Cybernetics, Part C (Applications and Reviews)*, 42(6):1291–1307, 2012.
- X. Guo, S. Singh, H. Lee, R. L. Lewis, and X. Wang. Deep learning for real-time atari game play using offline Monte-Carlo tree search planning. In Z. Ghahramani, M. Welling, C. Cortes, N. D. Lawrence, and K. Q. Weinberger, editors, *Advances in Neural Information Processing Systems 27*, pages 3338–3346. Curran Associates, Inc., 2014.
- X. Guo, S. Singh, R. Lewis, and H. Lee. Deep learning for reward design to improve Monte Carlo tree search in atari games. *arXiv preprint arXiv:1604.07095*, 2016.

- A. Gupta, R. Mendonca, Y. Liu, P. Abbeel, and S. Levine. Meta-reinforcement learning of structured exploration strategies. *arXiv preprint arXiv:1802.07245*, 2018.
- J. P. Hanna and P. Stone. Grounded action transformation for robot learning in simulation. In *Association for the Advancement of Artificial Intelligence*, pages 3834–3840, 2017.
- H. F. Harlow. Learning and satiation of response in intrinsically motivated complex puzzle performance by monkeys. *Journal of Comparative and Physiological Psychology*, 43(4):289, 1950.
- S. Harter. A new self-report scale of intrinsic versus extrinsic orientation in the classroom: Motivational and informational components. *Developmental Psychology*, 17(3):300, 1981.
- H. C. Herbol, W. Hu, P. Frazier, P. Clancy, and M. Poloczek. Efficient search of compositional space for hybrid organic–inorganic perovskites via Bayesian optimization. *NPJ Computational Materials*, 4(1):51, 2018.
- J. M. Hernández-Lobato, J. Requeima, E. O. Pyzer-Knapp, and A. Aspuru-Guzik. Parallel and distributed Thompson sampling for large-scale accelerated exploration of chemical space. In *International Conference on Machine Learning*, pages 1470–1479, 2017.
- X. Huang and J. Weng. Novelty and reinforcement learning in the value system of developmental robots. In *2nd International Workshop on Epigenetic Robotics: Modeling Cognitive Development in Robotic Systems*. Lund University Cognitive Studies, 2002.
- D. R. Jiang, E. Ekwedike, and H. Liu. Feedback-based tree search for reinforcement learning. In *International Conference on Machine Learning*, pages 2284–2293, 2018.
- D. R. Jones, M. Schonlau, and W. J. Welch. Efficient global optimization of expensive black-box functions. *Journal of Global optimization*, 13(4):455–492, 1998.
- F. Kaplan and P.-Y. Oudeyer. Maximizing learning progress: An internal reward system for development. In *Embodied Artificial Intelligence*, pages 259–270. Springer, 2004.
- M. Kearns and S. Singh. Near-optimal reinforcement learning in polynomial time. *Machine Learning*, 49(2-3):209–232, 2002.
- A. Klein, S. Falkner, S. Bartels, P. Hennig, and F. Hutter. Fast Bayesian optimization of machine learning hyperparameters on large datasets. *arXiv preprint arXiv:1605.07079*, 2016.
- G. Konidaris and A. Barto. Autonomous shaping: Knowledge transfer in reinforcement learning. In *International Conference on Machine Learning*, pages 489–496. ACM, 2006.

- G. Lample and D. S. Chaplot. Playing fps games with deep reinforcement learning. In *Association for the Advancement of Artificial Intelligence*, pages 2140–2146, 2017.
- L. Li, K. Jamieson, G. DeSalvo, A. Rostamizadeh, and A. Talwalkar. Hyperband: a novel bandit-based approach to hyperparameter optimization. volume 18, pages 6765–6816, 2017.
- D. J. Mankowitz, A. Židek, A. Barreto, D. Horgan, M. Hessel, J. Quan, J. Oh, H. van Hasselt, D. Silver, and T. Schaul. Unicorn: Continual learning with a universal, off-policy agent. *arXiv preprint arXiv:1802.08294*, 2018.
- L. Matthies, E. Gat, R. Harrison, B. Wilcox, R. Volpe, and T. Litwin. Mars microrover navigation: Performance evaluation and enhancement. *Autonomous robots*, 2(4):291–311, 1995.
- V. Mnih, K. Kavukcuoglu, D. Silver, A. Graves, I. Antonoglou, D. Wierstra, and M. Riedmiller. Playing atari with deep reinforcement learning. *arXiv preprint arXiv:1312.5602*, 2013.
- J. Močkus. On Bayesian methods for seeking the extremum. In *Optimization Techniques IFIP Technical Conference*, pages 400–404. Springer, 1975.
- E. E. Moodie, B. Chakraborty, and M. S. Kramer. Q-learning for estimating optimal dynamic treatment rules from observational data. *Canadian Journal of Statistics*, 40(4):629–645, 2012.
- I. Mordatch, N. Mishra, C. Eppner, and P. Abbeel. Combining model-based policy search with online model learning for control of physical humanoids. In *International Conference on Robotics and Automation*, pages 242–248. IEEE, 2016.
- P. Morere and F. Ramos. Bayesian rl for goal-only rewards. In *Conference on Robot Learning*, 2018.
- A. Nayebi, A. Munteanu, and M. Poloczek. A framework for Bayesian optimization in embedded subspaces. In *International Conference on Machine Learning*, pages 4752–4761, 2019.
- A. Y. Ng, D. Harada, and S. Russell. Policy invariance under reward transformations: Theory and application to reward shaping. In *International Conference on Machine Learning*, volume 99, pages 278–287, 1999.
- P. Nikolaev, D. Hooper, N. Perea-Lopez, M. Terrones, and B. Maruyama. Discovery of wall-selective carbon nanotube growth conditions via automated experimentation. *ACS Nano*, 8(10):10214–10222, 2014.
- J. Oh, X. Guo, H. Lee, R. L. Lewis, and S. Singh. Action-conditional video prediction using deep networks in atari games. In C. Cortes, N. D. Lawrence, D. D. Lee, M. Sugiyama, and R. Garnett, editors, *Advances in Neural Information Processing Systems 28*, pages 2863–2871. Curran Associates, Inc., 2015.

- I. Osband and B. Van Roy. Why is posterior sampling better than optimism for reinforcement learning? In *International Conference on Machine Learning*, pages 2701–2710. JMLR. org, 2017.
- I. Osband, D. Russo, and B. Van Roy. (More) Efficient reinforcement learning via posterior sampling. In C. J. C. Burges, L. Bottou, M. Welling, Z. Ghahramani, and K. Q. Weinberger, editors, *Advances in Neural Information Processing Systems 26*, pages 3003–3011. Curran Associates, Inc., 2013.
- I. Osband, B. Van Roy, and Z. Wen. Generalization and exploration via randomized value functions. *arXiv preprint arXiv:1402.0635*, 2014.
- I. Osband, C. Blundell, A. Pritzel, and B. Van Roy. Deep exploration via bootstrapped DQN. In D. D. Lee, M. Sugiyama, U. V. Luxburg, I. Guyon, and R. Garnett, editors, *Advances in Neural Information Processing Systems 29*, pages 4026–4034. Curran Associates, Inc., 2016.
- I. Osband, D. Russo, Z. Wen, and B. Van Roy. Deep exploration via randomized value functions. *arXiv preprint arXiv:1703.07608*, 2017.
- G. Ostrovski, M. G. Bellemare, A. v. d. Oord, and R. Munos. Count-based exploration with neural density models. *arXiv preprint arXiv:1703.01310*, 2017.
- D. Pathak, P. Agrawal, A. A. Efros, and T. Darrell. Curiosity-driven exploration by self-supervised prediction. In *International Conference on Machine Learning*, volume 2017, 2017.
- M. Poloczek, J. Wang, and P. Frazier. Multi-information source optimization. In *Advances in Neural Information Processing Systems*, pages 4288–4298, 2017.
- N. Prasad, L.-F. Cheng, C. Chivers, M. Draugelis, and B. E. Engelhardt. A reinforcement learning approach to weaning of mechanical ventilation in intensive care units. *arXiv preprint arXiv:1704.06300*, 2017.
- J. Randløv and P. Alstrøm. Learning to drive a bicycle using reinforcement learning and shaping. In *International Conference on Machine Learning*, volume 98, pages 463–471. Citeseer, 1998.
- C. E. Rasmussen and C. K. I. Williams. *Gaussian Processes for Machine Learning*. MIT Press, 2006. ISBN 0-262-18253-X.
- P. Redgrave and K. Gurney. The short-latency dopamine signal: A role in discovering novel actions? *Nature Reviews Neuroscience*, 7(12):967, 2006.
- M. B. Ring. *Continual learning in reinforcement environments*. PhD thesis, University of Texas at Austin, 1994.



- D. Russo and B. Van Roy. Learning to optimize via posterior sampling. *Mathematics of Operations Research*, 39(4):1221–1243, 2014.
- A. A. Rusu, M. Vecerik, T. Rothörl, N. Heess, R. Pascanu, and R. Hadsell. Sim-to-real robot learning from pixels with progressive nets. *arXiv preprint arXiv:1610.04286*, 2016.
- W. Schultz. Predictive reward signal of dopamine neurons. *Journal of Neurophysiology*, 80(1):1–27, 1998.
- W. Scott, P. Frazier, and W. Powell. The correlated knowledge gradient for simulation optimization of continuous parameters using gaussian process regression. *SIAM Journal on Optimization*, 21(3):996–1026, 2011.
- D. Silver, J. Schrittwieser, K. Simonyan, I. Antonoglou, A. Huang, A. Guez, T. Hubert, L. Baker, M. Lai, A. Bolton, et al. Mastering the game of Go without human knowledge. *Nature*, 550(7676):354, 2017.
- J. Snoek, H. Larochelle, and R. P. Adams. Practical Bayesian optimization of machine learning algorithms. In *Advances in Neural Information Processing Systems*, pages 2951–2959, 2012.
- J. Sorg, R. L. Lewis, and S. P. Singh. Reward design via online gradient ascent. In *Advances in Neural Information Processing Systems*, pages 2190–2198, 2010.
- J. Sorg, S. P. Singh, and R. L. Lewis. Optimal rewards versus leaf-evaluation heuristics in planning agents. In *Association for the Advancement of Artificial Intelligence*, 2011.
- B. C. Stadie, S. Levine, and P. Abbeel. Incentivizing exploration in reinforcement learning with deep predictive models. *arXiv preprint arXiv:1507.00814*, 2015.
- R. S. Sutton and A. G. Barto. *Reinforcement learning: An introduction*. MIT press, 2018.
- K. Swersky, J. Snoek, and R. P. Adams. Multi-task bayesian optimization. In *Advances in Neural Information Processing Systems*, pages 2004–2012, 2013.
- K. Swersky, J. Snoek, and R. P. Adams. Freeze-thaw Bayesian optimization. *arXiv preprint arXiv:1406.3896*, 2014.
- F. Tanaka and M. Yamamura. An approach to lifelong reinforcement learning through multiple environments. In *6th European Workshop on Learning Robots*, pages 93–99, 1997.
- H. Tang, R. Houthoofd, D. Foote, A. Stooke, O. X. Chen, Y. Duan, J. Schulman, F. DeTurck, and P. Abbeel. # exploration: A study of count-based exploration for deep reinforcement learning. In *Advances in Neural Information Processing Systems*, pages 2753–2762, 2017.

- A. C. Tenorio-Gonzalez, E. F. Morales, and L. Villaseñor-Pineda. Dynamic reward shaping: Training a robot by voice. In *Ibero-American Conference on Artificial Intelligence*, pages 483–492. Springer, 2010.
- S. Thrun, S. Thayer, W. Whittaker, C. Baker, W. Burgard, D. Ferguson, D. Hahnel, D. Montemerlo, A. Morris, Z. Omohundro, et al. Autonomous exploration and mapping of abandoned mines. *Robotics & Automation Magazine*, 11(4):79–91, 2004.
- R. Vuorio, D.-Y. Cho, D. Kim, and J. Kim. Meta continual learning. *arXiv preprint arXiv:1806.06928*, 2018.
- Z. Wang, C. Gehring, P. Kohli, and S. Jegelka. Batched large-scale Bayesian optimization in high-dimensional spaces. In *International Conference on Artificial Intelligence and Statistics*, pages 745–754, 2018.
- C. J. Watkins and P. Dayan. Q-learning. *Machine learning*, 8(3-4):279–292, 1992.
- C. J. C. H. Watkins. *Learning from delayed rewards*. PhD thesis, King’s College, Cambridge, 1989.
- A. Wilson, A. Fern, S. Ray, and P. Tadepalli. Multi-task reinforcement learning: A hierarchical Bayesian approach. In *International Conference on Machine Learning*, pages 1015–1022. ACM, 2007.
- C. Yu, M. Zhang, F. Ren, and G. Tan. Emotional multiagent reinforcement learning in spatial social dilemmas. *Transactions on Neural Networks and Learning Systems*, 26(12):3083–3096, 2015.
- Z. Zheng, J. Oh, and S. Singh. On learning intrinsic rewards for policy gradient methods. In *Advances in Neural Information Processing Systems*, pages 4649–4659, 2018.

## A Proof of Theorem 1

The proof follows the idea of Poloczek et al. (2017). We prove it for the case that allows different value of budget  $\tau$  during the training process.

Denote  $\mathcal{F}^n$  the  $\sigma$ -algebra generated by the history  $H^n$ . The expectation  $\mathbf{E}_n := \mathbf{E}[\cdot | \mathcal{F}^n]$  is taken with respect to  $\mathcal{F}^n$ . According to Frazier et al. (2009),

$$\mu^{n+1}(\theta, \tau) = \mu^n(\theta, \tau) + \tilde{\sigma}_n((\theta, \tau), (\theta^{n+1}, \tau^{n+1}, q^{n+1})) \cdot Z^{n+1}(\theta, \tau), \quad (7)$$

$$\begin{aligned} \Sigma^{n+1}((\theta', \tau'), (\theta, \tau)) &= \Sigma^n((\theta', \tau'), (\theta, \tau)) \\ &\quad - \tilde{\sigma}_{q^{n+1}}^n((\theta', \tau'), (\theta^{n+1}, \tau^{n+1}, q^{n+1})) \times \tilde{\sigma}_{q^{n+1}}^n((\theta, \tau), (\theta^{n+1}, \tau^{n+1}, q^{n+1})), \end{aligned} \quad (8)$$

where

$$\begin{aligned} Z^{n+1}(\theta, \tau) &= \frac{y^{n+1} - \mu_n(\theta, \tau)}{\sqrt{\text{Var}[y^{n+1} - \mu_n | \mathcal{F}^n]}}, \\ \tilde{\sigma}_q^n((\theta', \tau'), (\theta, \tau, q)) &= \frac{\Sigma^n((\theta', \tau'), (\theta, \tau))}{\sqrt{\lambda(\theta, \tau)/q + \Sigma^n((\theta, \tau), (\theta, \tau))}}. \end{aligned}$$

Therefore,

$$\begin{aligned} \mathbf{E}_n[\mu_{n+1}^* | \theta^{n+1} = \theta, \tau^{n+1} = \tau, q^{n+1} = q] \\ = \mathbf{E}_n[\max_{\theta'} \{\mu^n(\theta', \tau_{\max}) + \tilde{\sigma}_q^n((\theta', \tau_{\max}), (\theta, \tau, q)) \cdot Z^{n+1}\} | \theta^{n+1} = \theta, \tau^{n+1} = \tau, q^{n+1} = q], \end{aligned}$$

and the objective function can be written as

$$\frac{\text{GiS}^n(\theta', \tau', q')}{(q' \tau')} = \frac{1}{q' \tau'} \mathbf{E}_n[\max_{\theta''} \{A\} - \max_{\theta''} \mu^n(\theta'', \tau_{\max}) | \theta^{n+1} = \theta', \tau^{n+1} = \tau', q^{n+1} = q']. \quad (9)$$

where  $A = \mu^n(\theta'', \tau_{\max}) + \tilde{\sigma}_{q'}^n((\theta'', \tau_{\max}), (\theta', \tau', q')) \cdot Z^{n+1}$ .

Recall that  $\mu^n(\theta, \tau) = \mathbf{E}_n[f(\theta, \tau)]$ , and define

$$V_n(\theta, \tau, \theta', \tau') = \mathbf{E}_n[f(\theta, \tau) \cdot f(\theta', \tau')] = \Sigma^n((\theta, \tau), (\theta', \tau')) + \mu^n(\theta, \tau) \cdot \mu^n(\theta', \tau').$$

**Lemma 1** (Lemma 1 of Poloczek et al. (2017)). Let  $\tau, \tau' \in \mathcal{T}$  and  $\theta, \theta' \in \Theta$ . The limits of the series  $\{\mu^n(\theta, \tau)\}_n$  and  $\{V_n(\theta, \tau, \theta', \tau')\}_n$  exist. Denote them by  $\mu^\infty(\theta, \tau)$  and  $V_\infty(\theta, \tau, \theta', \tau')$  respectively. We have

$$\lim_{n \rightarrow \infty} \mu^n(\theta, \tau) = \mu^\infty(\theta, \tau) \quad (10)$$

$$\lim_{n \rightarrow \infty} V_n(\theta, \tau, \theta', \tau') = V_\infty(\theta, \tau, \theta', \tau') \quad (11)$$

almost surely. If  $(\theta', \tau')$  is sampled infinitely often, then  $\lim_{n \rightarrow \infty} V_n(\theta, \tau, \theta', \tau') = \mu^\infty(\theta, \tau) \cdot \mu^\infty(\theta', \tau')$ .

The following lemma states the asymptotic behavior of  $\text{GiS}^n(\theta', \tau', q')/(q'\tau')$  for  $n \rightarrow \infty$  as a function of  $\mu^n(\cdot, \cdot)$  and  $\tilde{\sigma}^n((\cdot, \cdot), (\cdot, \cdot, \cdot))$ .

**Lemma 2.** Let  $\tau' \in \mathcal{T}$ ,  $\theta' \in \Theta$ ,  $q' \in \mathcal{Q}$ , and suppose that  $\theta'$  is observed infinitely often with budget  $\tau'$  on an arbitrary sample path  $\omega$ . Then  $\tilde{\sigma}_{q'}^n((\theta'', \tau_{\max}), (\theta', \tau', q')) \rightarrow 0$  for every  $\theta'' \in \Theta$  and  $\text{GiS}^n(\theta', \tau', q')/(q'\tau') \rightarrow 0$  almost surely as  $n \rightarrow \infty$ .

*Proof.* Lemma 1 implies  $\Sigma^n((\theta, \tau), (\theta', \tau')) = \mathbf{E}_n[f(\theta, \tau) \cdot f(\theta', \tau')] - \mu^n(\theta, \tau) \cdot \mu^n(\theta', \tau') \rightarrow 0$  as  $n \rightarrow \infty$ . First suppose  $\lambda(\theta', \tau') = 0$  and that  $(\theta', \tau')$  is sampled for the first time in iteration  $m$ . According to (8),

$$\Sigma^{m+1}((\theta', \tau'), (\theta', \tau')) = \Sigma^m((\theta', \tau'), (\theta', \tau')) - \frac{[\Sigma^m((\theta', \tau'), (\theta', \tau'))]^2}{\Sigma^m((\theta', \tau'), (\theta', \tau'))} = 0.$$

Therefore for any  $(\theta, \tau)$ , we have

$$\begin{aligned} \mathbf{E}_{m+1}[f(\theta, \tau) \cdot f(\theta', \tau')] &= \mu^{m+1}(\theta, \tau) \cdot \mu^{m+1}(\theta', \tau'), \\ \Sigma^{m+1}((\theta, \tau), (\theta', \tau')) &= 0 \end{aligned}$$

according to Lemma 1, and

$$\text{GiS}^n(\theta', \tau', q')/(q'\tau') = 0$$

holds in iteration  $m + 1$  and all subsequent iterations according to (9).

Now suppose  $\lambda(\theta', \tau') > 0$ . Then for all  $\theta'' \in \Theta'$ , we have

$$\lim_{n \rightarrow \infty} \tilde{\sigma}_{q'}^n((\theta'', \tau_{\max}), (\theta', \tau', q')) = \lim_{n \rightarrow \infty} \frac{\Sigma^n((\theta'', \tau_{\max}), (\theta', \tau'))}{\sqrt{\lambda(\theta', \tau')/q' + \Sigma^n((\theta', \tau'), (\theta', \tau'))}} = 0.$$

Recall that  $\{\mu^n(\theta', \tau')\}_n$  and  $\{\tilde{\sigma}_{q'}^n((\theta'', \tau_{\max}), (\theta', \tau', q'))\}_n$  are uniformly integrable (u.i.) families of random variables that converge a.s. to their respective limits  $\mu^\infty(\theta', \tau')$  and  $\tilde{\sigma}_{q'}^\infty((\theta'', \tau_{\max}), (\theta', \tau', q')) = 0$ . Thus,

$$\begin{aligned} & \lim_{n \rightarrow \infty} \frac{\text{GiS}^n(\theta', \tau', q')}{q' \tau'} \\ &= \frac{1}{q' \tau'} \left[ \int_{-\infty}^{+\infty} \phi(Z) \cdot \max_{\theta'' \in \Theta'} \{ \mu^\infty(\theta'', \tau_{\max}) + \tilde{\sigma}_{q'}^\infty((\theta'', \tau_{\max}), (\theta', \tau', q')) \cdot Z \} dZ - \max_{\theta'' \in \Theta'} \mu^n(\theta'', \tau_{\max}) \right] \\ &= 0, \end{aligned}$$

where we used that  $\{\tilde{\sigma}_{q'}^n((\theta'', \tau_{\max}), (\theta', \tau', q')) \cdot Z\}_n$  is u.i. since  $\{Z\}_n$  and  $\{\tilde{\sigma}_{q'}^n((\theta'', \tau_{\max}), (\theta', \tau', q'))\}_n$  are independent, the sum of u.i. random variables is u.i., and so is the maximum over a finite collection of u.i. random variables.  $\square$

Recall that BESD picks  $(\theta^{n+1}, \tau^{n+1}, q^{n+1}) \in \arg \max_{\theta, \tau, q} \text{GiS}^n(\theta, \tau, q)/(q\tau)$  in each iteration  $n$ . Since  $f(\theta', \tau')$  is sampled infinitely often (by choice of  $\theta', \tau'$ ),  $\text{GiS}^n(\theta, \tau, q)/(q\tau) \rightarrow 0$  holds almost surely for all  $\tau \in \mathcal{T}$ ,  $q \in \mathcal{Q}$  and  $\theta \in \Theta'$ .

**Lemma 3.** *If  $\lim_{n \rightarrow \infty} \text{GiS}^n(\theta, \tau, q)/(q\tau) = 0$  holds for all  $\theta, \tau, q$ , then  $\arg \max_{\theta \in \Theta'} \mu^\infty(\theta, \tau_{\max}) = \arg \max_{\theta \in \Theta'} f(\theta, \tau_{\max})$  holds almost surely.*

*Proof.* Lemma 1 gives that  $\lim_{n \rightarrow \infty} \Sigma_n((\theta, \tau_{\max}), (\theta, \tau_{\max})) = \Sigma^\infty((\theta, \tau_{\max}), (\theta, \tau_{\max}))$  a.s. for all  $\theta \in \Theta'$ . First note that a maximizer is known perfectly if the posterior variance  $\Sigma^\infty((\theta, \tau_{\max}), (\theta, \tau_{\max})) = 0$  for all  $\theta \in \Theta'$ . Thus, define  $\hat{\Theta} = \{\theta \in \Theta' \mid \Sigma^\infty((\theta, \tau_{\max}), (\theta, \tau_{\max})) > 0\}$  and let  $\hat{\theta} \in \hat{\Theta}$ . Then

$$\tilde{\sigma}_{q_{\max}}^\infty((\hat{\theta}, \tau_{\max}), (\hat{\theta}, \tau_{\max}, q_{\max})) = \frac{\Sigma^\infty((\hat{\theta}, \tau_{\max}), (\hat{\theta}, \tau_{\max}))}{\sqrt{\lambda(\hat{\theta}, \tau_{\max})/q_{\max} + \Sigma^\infty((\hat{\theta}, \tau_{\max}), (\hat{\theta}, \tau_{\max}))}} > 0. \quad (12)$$

Note that  $\text{GiS}^\infty(\hat{\theta}, \tau_{\max}, q_{\max}) / (q_{\max} \tau_{\max}) > 0$  if there are  $\theta_1, \theta_2 \in \Theta'$  with

$$\tilde{\sigma}_{q_{\max}}^\infty((\theta_1, \tau_{\max}), (\hat{\theta}, \tau_{\max}, q_{\max})) \neq \tilde{\sigma}_{q_{\max}}^\infty((\theta_2, \tau_{\max}), (\hat{\theta}, \tau_{\max}, q_{\max})).$$

The reason is that then there is a  $Z_0$  such that w.l.o.g. for all  $Z > Z_0$ ,

$$\begin{aligned} & \mu^\infty(\theta_1, \tau_{\max}) + \tilde{\sigma}_{q_{\max}}^\infty((\theta_1, \tau_{\max}), (\hat{\theta}, \tau_{\max}, q_{\max})) \cdot Z \\ & > \mu^\infty(\theta_2, \tau_{\max}) + \tilde{\sigma}_{q_{\max}}^\infty((\theta_2, \tau_{\max}), (\hat{\theta}, \tau_{\max}, q_{\max})) \cdot Z \end{aligned}$$

(and vice versa for  $Z < Z_0$ ), resulting in a strictly positive numerator of (9). Thus,  $\frac{\text{GiS}^\infty(\hat{\theta}, \tau_{\max}, q_{\max})}{(q_{\max} \tau_{\max})} = 0$  implies  $\tilde{\sigma}_{q_{\max}}^\infty(\theta'', \hat{\theta}, \tau_{\max}) = \tilde{\sigma}_{q_{\max}}^\infty(\hat{\theta}, \hat{\theta}, \tau_{\max})$  for all  $\theta'' \in \Theta'$ , or equivalently for all  $\theta'', \theta''' \in \Theta'$ ,

$$\frac{\Sigma^\infty((\theta''', \tau_{\max}), (\hat{\theta}, \tau_{\max}))}{\sqrt{\lambda(\hat{\theta}, \tau_{\max})/q_{\max} + \Sigma^\infty((\hat{\theta}, \tau_{\max}), (\hat{\theta}, \tau_{\max}))}} = \frac{\Sigma^\infty((\theta'', \tau_{\max}), (\hat{\theta}, \tau_{\max}))}{\sqrt{\lambda(\hat{\theta}, \tau_{\max})/q_{\max} + \Sigma^\infty((\hat{\theta}, \tau_{\max}), (\hat{\theta}, \tau_{\max}))}}.$$

Moreover, (12) implies

$$\lambda(\hat{\theta}, \tau_{\max})/q_{\max} + \Sigma^\infty((\hat{\theta}, \tau_{\max}), (\hat{\theta}, \tau_{\max})) > 0,$$

and hence  $\Sigma^\infty((\theta''', \tau_{\max}), (\hat{\theta}, \tau_{\max})) = \Sigma^\infty((\theta'', \tau_{\max}), (\hat{\theta}, \tau_{\max}))$ . Thus, the covariance matrix of  $\{f(\theta, \tau_{\max}) | \theta \in \Theta'\}$  is proportional to the all-ones matrix, and hence  $f(\theta, \tau_{\max}) - \mu^{(\infty)}(\theta, \tau_{\max})$  is a normal random variable that is constant across all  $\theta \in \Theta'$ . Therefore,  $\arg \max_{\theta \in \Theta'} \mu^{(\infty)}(\theta, \tau_{\max}) = \arg \max_{\theta \in \Theta'} f(\theta, \tau_{\max})$  holds. It follows that a maximizer of  $f(\cdot, \tau_{\max})$  over  $\Theta'$  is perfectly known (but not necessarily its exact objective value).  $\square$

## B Baseline Algorithm Descriptions

1. The first baseline is the Q-Learning (QL) algorithm of [Watkins \(1989\)](#) with no subgoals or reward shaping: that is, we directly run QL on environment  $\xi^{N+1}$  for  $\tau_{\max}$  interactions. The reported results are average performances over 200 realizations of  $\xi^{N+1}$  for each domain.
2. The ‘‘transfer’’ Q-learning (TQL) is based on QL, with Q-matrices stored after training. For the test instance, QL is started from a randomly chosen previously stored matrix.

3. The popular Hyperband (HB) algorithm of Li et al. (2017) treats hyperparameter optimization as a pure-exploration infinite-armed bandit problem; it uses sophisticated techniques for adaptive resource allocation and early-stopping to concentrate its learning efforts on promising designs. Setting  $\eta = 3$  (the default value) and  $R = 81$ , HB consists of  $\lfloor \log_\eta R \rfloor$  rounds. The first round starts with  $R$  samples of subgoal designs  $\theta$  from a Latin hypercube sample. Each  $\theta$  is evaluated for  $\tau_{\min}$  steps and then only the best  $1/\eta$ -fraction designs are kept for the next round. In round  $i$ , Hyperband samples  $R/\eta^{i-1}$  subgoal designs to evaluate for  $\tau_{\min} \eta^{i-1}$  steps.
4. The expected improvement (EI) algorithm (Moćkus, 1975; Jones et al., 1998) is the most popular BO method. EI allocates one sample in each round, selecting a point that maximizes the expected improvement beyond currently sampled points:  $\theta^{n+1} = \arg \max_{\theta} \mathbf{E}_n [[y(\theta, \tau_{\max}) - \mu_n^*]^+]$ . In each iteration, we evaluate the EI selection using  $\tau_{\max}$  iterations. EI is implemented in Python 2.7 using the GPyOpt package (González, 2016).
5. The lower-confidence-bound (LCB) algorithm (Cox and John, 1992) controls the exploration-exploitation trade-off using a “bonus term” proportional to the standard deviation at each point:  $\text{LCB}(\theta) = \mu(\theta, \tau_{\max}) - \kappa \sqrt{\lambda(\theta, \tau_{\max})}$ . The parameter  $\kappa$  is set to 2. LCB is also implemented in Python 2.7 using the GPyOpt package (González, 2016).

## C Benefits of BESD Recommendations

Table 1 displays the ratio of the scores of an agent using subgoals versus an agent learning from scratch. The implemented subgoal is one particular recommendation of BESD. GW10, TR, MC, KEY2, KEY3 and GW20 are measured per 100, 200, 1000, 500, 500 and 1000 steps respectively. The agent’s task in all of the environments except for TR is to reach the goal as quickly as possible. The performance is measured by the mean number of steps that the agent takes from start to goal. Thus, a smaller ratio reflects the advantage of the recommended subgoal design  $\theta$ . In TR, the agent’s task is to maximize reward (rather than to minimize steps), hence here a large ratio indicates improvements for TR and shows the benefits of BESD.

Table 1: The performance ratios of the agent using subgoals versus the standard agent

No.	GW10	TR	MC	KEY2	KEY3	GW20
1	0.458	0.436	0.980	1.456	1.025	0.779
2	0.218	2.823	1.048	0.736	0.940	0.492
3	0.086	2.823	0.949	1.277	0.698	0.234
4	0.080	0.917	0.896	0.704	0.788	0.224
5	0.070	6.723	0.987	1.355	0.531	0.108
6	0.086	8.939	0.878	0.856	0.503	0.088
7	0.080	9.908	1.077	0.920	0.623	0.068
8	0.087	10.216	0.877	0.883	0.532	0.075
9	0.069	23.2936	0.512	0.232	0.566	0.059
10	0.069	18.011	0.354	0.332	0.361	0.058

## D Hyperparameter Estimation

The hyperparameters of the covariance function  $k$  are set via *maximum a posteriori* (MAP) estimation. Recall that a MAP estimate is the mode under the log-posterior obtained as the sum of the log-marginal likelihood of the observations and the logarithm of the probability under a hyper-prior. We focus on describing the hyper-prior, since the log-marginal likelihood follows canonically; see (Rasmussen and Williams, 2006, Ch. 5) for details. The proposed prior extends the hyper-prior for the multi-task GP model used in (Poloczek et al., 2017). We set the mean function  $\mu$  and the noise function  $\lambda$  to constants. For the covariance function we need to estimate  $d + 5$  hyperparameters: the signal variance, one length scale for every subgoal parameter in  $\theta$  and the four parameters associated with  $k_\tau$ . We suppose a normal prior for these parameters. For the signal variance, the prior mean is given by the variance of the observations, after subtracting the above estimate for the observational noise. Here we use the independence of observational noise that we argued above. For any length scale, we set the prior mean to the size of the interval that the associated parameter is chosen in. Having determined a prior mean  $\mu_\psi$  for each hyperparameter  $\psi$ , we may then set the variance of the normal prior to  $\sigma_\psi^2 = (\mu_\psi/2)^2$ .

## E Acquisition Value Computation

This section details how to find the maximum GiS per effort on the testing MDP in period  $n$  efficiently. This approach follows (Scott et al., 2011). Note that any finite set of designs  $\{(\theta, \tau, q)\}_n$ ,



each describing subgoals, number of steps and of replications, has a joint multivariate normal distribution under the posterior given the history at time  $H^n$ , thus  $\mu_{n+1}^*(\theta) = \mathbf{E}_{n+1}[f(\theta, \cdot)]$  can be written as

$$\mu_{n+1}^*(\theta) = \mu_n^*(\theta) + \tilde{\sigma}_n((\theta, \tau_{\max}), (\theta^{n+1}, \tau^{n+1}, q^{n+1})) \cdot Z^{n+1},$$

where  $Z^{n+1}$  is a standard normal random variable and

$$\begin{aligned} & \tilde{\sigma}_n^2((\theta, \tau_{\max}), (\theta^{n+1}, \tau^{n+1}, q^{n+1})) \\ &= \text{Var}_n[g(\theta, \tau_{\max})] - \mathbf{E}_n[\text{Var}_{n+1}[g(\theta, \tau_{\max})] \mid \theta^{n+1}, \tau^{n+1}, q^{n+1}] \end{aligned} \quad (13)$$

quantifies the effect that the observation at  $(\theta^{n+1}, \tau^{n+1}, q^{n+1})$  has on the posterior distribution of  $\theta$ . Note that  $q^{n+1}$  only affects the amount of noise for the next observation but is not a coordinate of the latent function over the rewards. Recall that  $\Theta'$  is a discrete set that  $\Theta' \subseteq \Theta$ ,  $|\Theta'| = L < \infty$ . We take the maximum in GiS per effort over these  $L$  points as an approximation:

$$\begin{aligned} \text{GiS}^n(\theta, \tau, q) &\approx \mathbf{E}_n \left[ \max_{\theta' \in \Theta'} \mu^n(\theta', \tau_{\max}) + \tilde{\sigma}_n((\theta, \tau_{\max}), (\theta^{n+1}, \tau^{n+1}, q^{n+1})) Z^{n+1} \right] - \max_{\theta' \in \Theta'} \mu(\theta', \tau_{\max}) \\ &= h(\mu^n(\Theta', \tau_{\max}), \tilde{\sigma}_n(\Theta', \theta^{n+1}, \tau^{n+1}, q^{n+1})), \end{aligned}$$

where

$$\begin{aligned} \mu^n(\Theta', \tau_{\max}) &= (\mu^n(\theta_i, \tau_{\max}))_{i=1}^L, \\ \tilde{\sigma}_n(\Theta', \theta^{n+1}, \tau^{n+1}, q^{n+1}) &= (\tilde{\sigma}_n(\theta_i, \theta^{n+1}, \tau^{n+1}, q^{n+1}))_{i=1}^L, \end{aligned}$$

and function  $h : \mathbb{R}^L \times \mathbb{R}^L \rightarrow \mathbb{R}$  is defined by  $h(a, b) = \mathbf{E}[\max_i a_i + b_i Z] - \max_i a_i$ , where  $a$  and  $b$  are any deterministic vectors, and  $Z$  is a one-dimensional standard normal random variable. Denote  $\mu^n(\theta_i, \tau_{\max})$  and  $\tilde{\sigma}_n(\theta_i, \theta^{n+1}, \tau^{n+1}, q^{n+1})$  by  $\dot{\mu}_i$  and  $\dot{\sigma}_i$  respectively for short.

Based on Algorithm 1 in (Frazier et al., 2009) and the evaluation of  $h(a, b)$ , we can get a set of  $k$  indices  $\{j_1, j_2, \dots, j_k\} \in \{1, 2, \dots, L\}$  such that

$$\text{GiS}^n(\theta, \tau, q) = \sum_{i=1}^{k-1} (\dot{\sigma}_{j_{i+1}} - \dot{\sigma}_{j_i}) f \left( - \left| \frac{\dot{\mu}_{j_{i+1}} - \dot{\mu}_{j_i}}{\dot{\sigma}_{j_{i+1}} - \dot{\sigma}_{j_i}} \right| \right),$$

where  $f(z) = \varphi(z) + z\Phi(z)$  with  $\varphi$  and  $\Phi$  being the standard normal cdf and pdf. This shows how to compute the gain in score. To get the GiS per effort, we divide both sides by the budget  $(\tau^{n+1} \cdot q^{n+1})$ , which is the number of replications multiplied with the number of steps of the underlying RL policy in each replication.